Journal of Associated Medical Sciences 2023; 56 (3): 96-104

JAMS
Journal of Associated Medical Sciences

Scopus Indexed & Thai-Journal Citation Index Centre (TCI)

Journal of Associated Medical Sciences

Journal homepage: https://www.tci-thaijo.org/index.php/bulletinAMS/index

The usefulness of the modified deep convolutional neural network model in improving the detection of COVID-19 on chest X-ray images

Titipong Kaewlek* **Thunyarat Chusin Sumalee Yabsantia Nuntawat Udee**

Department of Radiological Technology, Faculty of Allied Health Sciences, Naresuan University, Phitsanulok Province, Thailand.

ARTICLE INFO

Article history:
Received 9 May 2023
Accepted as revised 14 July 2023
Available online 16 July 2023

Keywords:
Artificial intelligence, convolutional neural network, COVID-19, chest X-ray, deep learning

ABSTRACT

Background: The COVID-19 pandemic has rapidly spread worldwide, leading to a global health crisis. Although the real-time polymerase chain reaction (RT-PCR) test is highly specific and sensitive in detecting COVID-19, chest X-rays have emerged as an optional diagnostic tool for COVID-19-induced lung lesions. Artificial intelligence (AI), particularly deep learning, is a rapidly evolving field with significant potential in medical image analysis, including the quick detection of COVID-19 to improve accuracy.

Objectives: This study aims to enhance the accuracy of COVID-19 image detection on chest X-ray images by modifying the deep convolutional neural network.

Materials and methods: We conducted lung segmentation and COVID-19 image classification experiments using a dataset of chest X-rays. The U-net algorithm was utilized for lung segmentation of COVID-19 and non-COVID-19 images. We developed a Modified Deep Convolutional Neural Network (MD-CNN) to classify the two image classes. The MD-CNN model was compared with two other models, ResNet and AlexNet, and evaluated for accuracy, sensitivity (recall), specificity, positive predictive value (precision), F1-score, and area under the curve (AUC).

Results: Our experimental results demonstrate that the MD-CNN model achieved an accuracy of 97.95%, outperforming ResNet and AlexNet, which achieved 90.25% and 78.95%, respectively. The MD-CNN model also exhibited better sensitivity, F1-score, and AUC than the other models, while its specificity and precision were comparable to those of the ResNet model.

Conclusion: The proposed MD-CNN model demonstrates significant potential for high accuracy in COVID-19 image detection compared to ResNet and AlexNet. It can serve as a useful tool for radiologists in the COVID-19 screening process, potentially reducing the workload, and improving the efficiency of COVID-19 diagnosis.

Introduction

The infectious Coronavirus (COVID-19) has spread worldwide, and as of April 3, 2023, the World Health Organization (WHO) has reported 762,201,169 confirmed cases of COVID-19, including 6,893,190 deaths.[1] The highly specific and sensitive tool for diagnosing the COVID-19 virus is real-time polymerase chain reaction (RT-PCR). However, WHO recommends reliable and accurate self-testing tools, such as SARS-CoV-2 Ag-RDTs, for self-testing for the COVID-19 virus.[2]

During the COVID-19 pandemic, chest X-rays and computed tomography are imaging instruments used to

* **Corresponding contributor.**
Author's Address: *Department of Radiological Technology, Faculty of Allied Health Sciences, Naresuan University, Phitsanulok Province, Thailand.*
E-mail address: titipongk@nu.ac.th
doi: 10.12982/JAMS.2023.059
E-ISSN: 2539-6056

classify the types of lung diseases, such as tuberculosis, pneumonia, and COVID-19.[3] Ground glass appearance indicates increased whiteness due to dense density and progresses to consolidation with the complete loss of lung markings on the lung.[4] Anterior-posterior (AP) positioning of chest X-ray on a portable machine produces poor image quality compared to posterior-anterior (PA) chest imaging demonstrated in dedicated radiography facilities. The chest radiograph may appear normal in up to 63% of COVID-19 cases, while 1-3% may present nodules, pneumothorax, or pleural effusion that might be incidental, caused by COVID-19, or comorbidities such as tumors or emphysema.[4] Computer-aided diagnosis (CAD) is an artificial intelligence that helps prove the efficiency of radiologist diagnostics.[5] Common applications include the detection of cancer on mammograms[6] and lesions on chest images[7]. Machine learning and deep learning are two techniques used for classifying pathology or the class of image lesions in radiology[8].

Deep learning enables automatic lesion detection and image classification. Various studies have employed convolutional neural networks (CNNs) for image classification, with research indicating the effective and accurate diagnostic potential of CNNs for COVID-19.[9-11] However, the application of image augmentation techniques to enhance performance is limited by the constraints of a small dataset.

The integration of CNN and recurrent neural network (RNN) replaced the fully connected layers with an RNN model, presenting the combined model with high accuracy.[12] However, it is not suitable for low-resource devices with a minimum of 19 GB RAM consumption for model training. Another work introduced BasicCovn Architecture with Log Scaling, which classified COVID-19 with 95.8% accuracy, 0.989 AUC, and suggested splitting techniques, such as k-fold data splitting, that could improve effective training.[13] The development of the CNN model remains a challenge for classifying COVID-19 images by chest X-ray because of the difficulty in identifying the tissue. The objective of this study is to modify deep convolutional neural networks (MD-CNN) and compare them with two models (ResNet, AlexNet) in classifying images of COVID-19 and normal chest X-rays.

Materials and methods

This study consists of three sections: the first is lung segmentation on chest X-ray images, the second is COVID-19 and non-COVID-19 image classification, and the third is the evaluation of the performance of three models.

Lung segmentation

Dataset for lung segmentation study

We collected a total of 704 chest X-ray images containing chest X-ray images and mask images. These images were separated into two sets: a training set consisting of 563 images and a testing set consisting of 141 images. An example image is shown in Figure 1. The images were acquired from Kaggle, which obtained them from the Montgomery County X-ray Set.[14] The images were in Portable Network Graphics (PNG) format with 8 bits, and the image size was 256 x 256 pixels.

U-Net architecture for lung segmentation

The architecture of the U-Net model used in this study is shown in Figure 2.[15] The input consists of 704 images (256x256x1 pixel) processed by the U-Net model. The model consists of a contracting path and an expansive path. The contracting path follows the typical architecture of a convolutional network, with the repeated application of two 3x3 convolutions (unpadded convolutions), each followed by a rectified linear unit (ReLU) and a 2x2 max pooling operation with stride 2 for downsampling. At each downsampling step, the number of feature channels is doubled. Every step in the expansive path consists of an upsampling of the feature map followed by a 2x2 convolution (up-convolution) that halves the number of feature channels, a concatenation with the correspondingly cropped feature map from the contracting path, and two 3x3 convolutions, each followed by a ReLU. The cropping is necessary due to the loss of border pixels in every convolution. At the final layer, a 1x1 convolution is followed by a sigmoid.

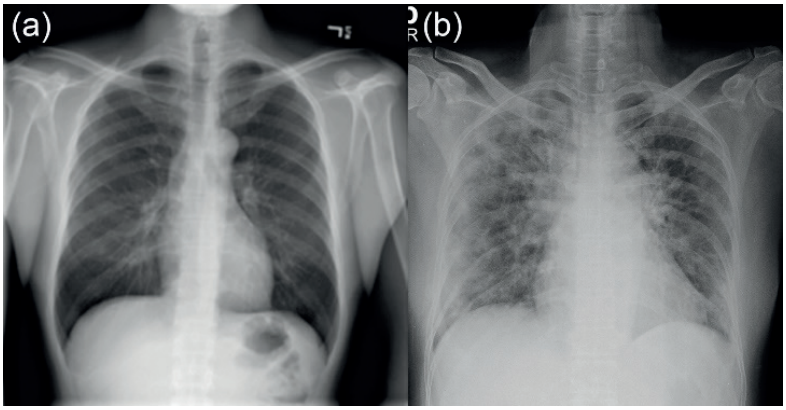

Figure 1 *Example image.*
(a: normal, b: CIVID-19 radiography)

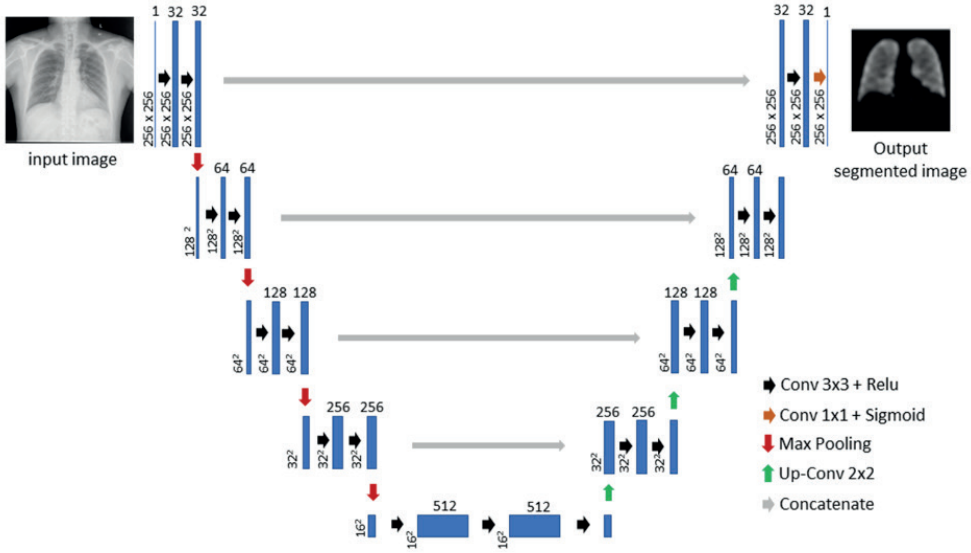

Figure 2 *U-Net architecture of this study.*

The image segmentation model was trained using a learning rate of 0.2 with a lower bound on a learning rate of 0.000001. The network training was set to a batch size of 32 for 70 epochs. The trained model was used to segment the lung region of the initial image in the image classification section.

The Dice similarity coefficient (DSC) was used to analyze the similarity between mask images and predicted segmentations, as shown in Equation 1.

$$DSC = A \cap B / (|A| + |B|) \quad (1)$$

A is the mask area, *B* is the segmentation predicted area.

Dataset for image classification

A total of 20,000 chest X-ray images were collected, including 10,000 images labelled as COVID-19 (COVID) and 10,000 images labelled as normal (non-COVID-19). These images were randomly selected from the Kaggle dataset and segmented using the U-Net architecture for lung segmentation.[16]

Proposed image classification model: The modified deep convolutional neural network (MD-CNN)

The proposed model for the modified deep convolutional neural network (MD-CNN) architecture is shown in Figure 3. The proposed model differs from the conventional CNN in several aspects, including the input image size, the number of blocks for the convolutional layer, the dense layer, and the dropout rate. The overall parameters of the model are 4,947,162, which are all trainable. The model's details are as follows: the input layer receives 256x256x1. The feature extraction step consists of five blocks for the convolutional layer with a ReLU function, followed by a MaxPooling layer. The first and second blocks have two convolutional layers (3x3) with a ReLU function and are followed by a MaxPooling layer (2x2), while the third to fifth blocks have three convolutional layers (3x3) with a ReLU function followed by a MaxPooling layer (3x3). The output of feature extraction is sent to a flattened layer to convert the image data to a one-dimensional vector. The classification part of the proposed model consists of two dense layers (512), followed by a 0.2 dropout layer, and the last dense layer

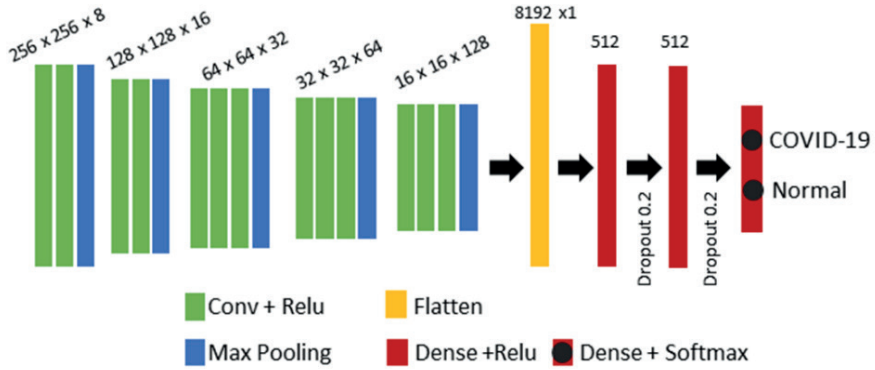

Figure 3 *The proposed model architecture.*

with SoftMax activation function produced four neurons that classify the output into two groups of image classes: COVID-19 and non-COVID-19.

To compare the performance of the proposed model, two models (ResNet and AlexNet) were selected in terms of their performance. Information on ResNet and AlexNet is shown below.

ResNet model

The input layer receives 256x256x1 images. The feature extraction step consists of five blocks. The first block has a convolutional layer with a batch normalization layer, followed by the Relu function layer, and then a MaxPooling layer. The second to fifth layers have a ResNet block layer with different filter sizes, followed by the Global Average Pooling layer. The classification layer includes a dense layer with SoftMax activation function, producing four neurons that classify the output into two groups of image classes: COVID-19 and non-COVID-19.

AlexNet model

The input layer receives 256x256x1 images. The feature extraction step consists of five blocks. The first and second blocks have a convolutional layer with a Relu function, followed by a batch normalization layer, and then a MaxPooling layer. The third and fourth blocks have a convolutional layer with a Relu function. The fifth block has a convolutional layer with a Relu function, a batch normalization layer, followed by the MaxPooling layer. The output of feature extraction is sent to a flattened layer to convert image data into a one-dimensional vector. The classification layer includes two dense layers (4096) with Relu, and the second dense layer is followed by a 0.5 dropout layer. The output layer is processed by a dense layer with SoftMax activation function, producing four neurons that classify the output into two groups of image classes: COVID-19 and non-COVID-19.

Training image classification process

The image classification dataset is separated into three sets, consisting of 14,000 images for the train set, 4,000 images for the validation set, and 2,000 images for the test set. The train set images are trained by three models (MD-CNN, ResNet, and AlexNet), set to a batch size of 32 for 70 epochs. The validation set uses the same parameters as the training process. All processes run on Google Colaboratory (Tesla P100-PCIE: GPU).[17]

Statistical analysis

The two-confusion matrix, which classifies two types of chest X-ray images (COVID-19 and non-COVID-19), describes the performance of a classifier in four terms:

True Positives (TP): the model detects correctly classified COVID-19 images.

True Negatives (TN): the model detects non-COVID-19 images on non-COVID-19 images.

False Positives (FP): the model detects COVID-19 images on non-COVID-19 images.

False Negatives (FN): the model detects non-COVID-19 images on COVID-19 images.

The performance of models is evaluated using a confusion matrix. Statistical analysis: The accuracy, sensitivity (recall), specificity, positive predictive value (precision), and F1-score are given in equations (2)-(6). The receiver operating characteristic curves (ROC) and area under curves (AUC) are also evaluated.

$$\text{Accuracy} = \frac{TP+TN}{TP+TN+FP+FN} \quad (2)$$

$$\text{Positive predictive value(precision)} = \frac{TP}{TP+FP} \quad (3)$$

$$\text{Sensitivity (recall)} = \frac{TP}{TP+FN} \quad (4)$$

$$\text{Specificity} = \frac{TN}{TN+FP} \quad (5)$$

$$\text{F1 - score} = 2 \times \frac{\text{precision} \times \text{recall}}{\text{precision} + \text{recall}} \quad (6)$$

Results

Figure 4 shows the learning accuracy of the training and validation of the proposed method (MD-CNN). The accuracy of the training set reaches 0.95 after 10 epochs, while the accuracy of the validation set fluctuates between 30 and 60 epochs. The accuracy of the ResNet model at the training phase reaches 0.9879, while it is 0.7689 for the AlexNet model.

Lung segmentation

Figure 5 shows the performance of the U-Net for lung segmentation. The Dice similarity coefficient (DSC) indicates the high efficiency of U-Net. Therefore, the lung region in the images used for image classification was completely segmented for the learning of the three models.

Performance evaluation of COVID-19 and non-COVID-19 image classification

Table 1 shows the confusion matrix of the three models. The number of true positive images in the proposed model was equal to that of ResNet and higher than that of AlexNet. Additionally, the true negative of the proposed model was higher than that of both ResNet and Alex.

Figure 6 shows the performance of three models, including accuracy, sensitivity, F1-score, and the area under curve (AUC). The proposed model's accuracy, sensitivity, and AUC were significantly higher than ResNet and AlexNet. However, the specificity and precision of the ResNet model were slightly higher than those of the proposed model.

Figure 7 shows the receiver operating characteristic curves and area under the curves of three models. The curve of the proposed model is closely located in the top-left corner, indicating that the proposed model has the best performance with an AUC equal to 0.9788. The second-best performance was achieved by the ResNet model (AUC = 0.9184), and the AlexNet model had the lowest performance (AUC = 0.7957).

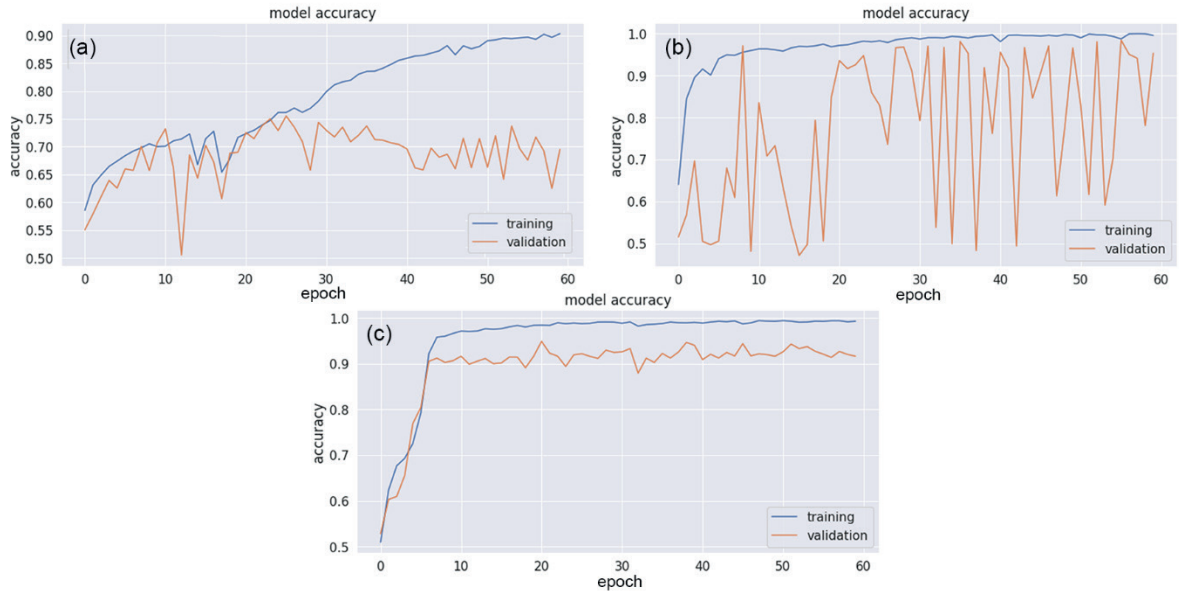

Figure 4 *Accuracy of the training and validation phase.*
(a: AlexNet, b: ResNet, c: the proposed method)

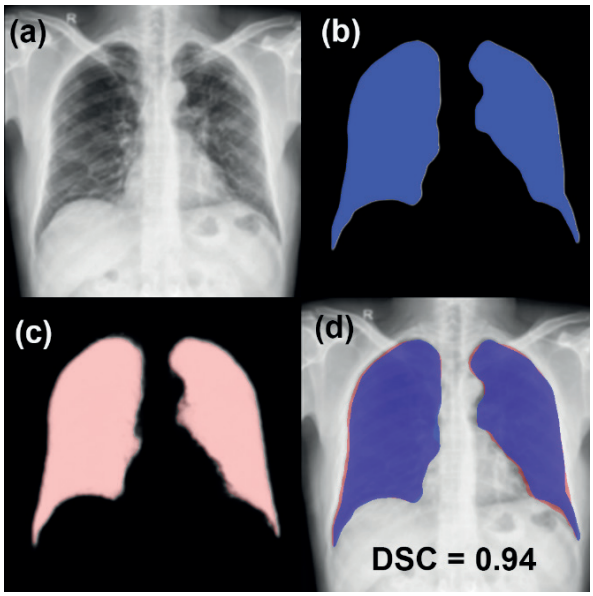

Figure 5 *The lung segmentation using U-Net.*
(a: the initial CXR image, b: ground truth mark (blue), c: the segmented predict (pink),
d: the overlap of (b) and (c) on (a) with an average of Dice similarity coefficient = 0.94)

Table 1 Confusion matrix of three models

Models	TP	FP	FN	TN
Proposed method	966	34	7	993
ResNet	1,000	0	195	805
AlexNet	862	138	283	717

*TP: true positive, FP: false positive, FN: false negative, TN: true negative

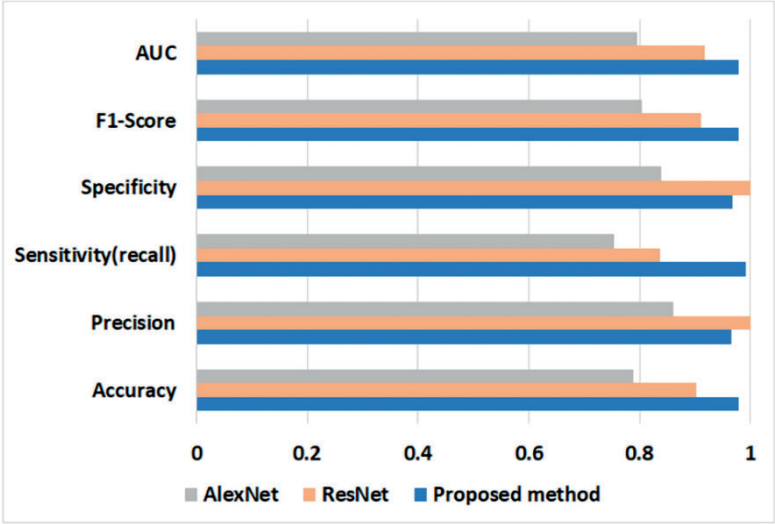

Figure 6 *The performance of three models including accuracy, precision, sensitivity, specificity, F1-score, and are under curve.*

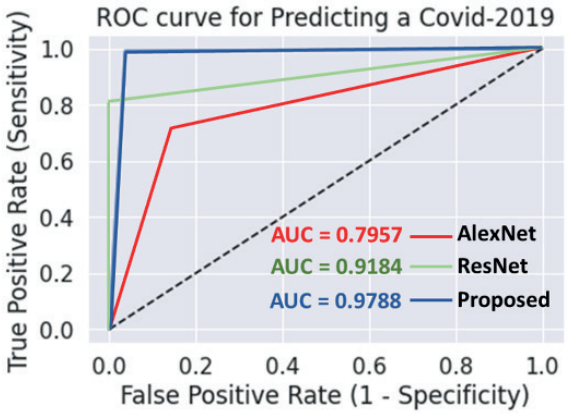

Figure 7 *Comparison of ROC and AUC of AlexNet, RetNet, and the proposed model.*

Discussion

This study consists of two sections including lung segmentation by U-net and image classification by three models (the proposed MD-CNN model, ResNet, and AlexNet). Lung segmentation is one factor that affects the efficiency of image classification on chest X-rays, which can be estimated by the Dice similarity coefficient (DSC) value. The DSC value shows the performance of image segmentation, with an ideal value of 1 indicating perfect segmentation. In this study, the average DSC was equal to 0.94, indicating that U-net can completely segment the lung region. Figure 5(d) shows the predicted lung segmentation closely overlapping the lung ground truth marks area in Figure 5(c).

To modify the convolutional neural network (CNN), we adapted the network structure including five blocks for feature extraction, a fully connected layer consisting of a flattened layer followed by two dense layers and 0.2 dropouts, and the last classification layer using Softmax activation function for classifying two-class images. The MD-CNN structure is very simple and highly performing compared to ResNet.

The accuracy, sensitivity, F1-score, and area under the curve of the proposed MD-CNN model were the highest (97.95%, 99.28%, 97.92%, and 0.98 AUC, respectively). The second-best was the ResNet model (90.25%, 83.68%, 91.12%, and 0.92 AUC, respectively). The lowest was the AlexNet model (78.95%, 75.28%, 80.37%, and 0.79 AUC, respectively). The precision and specificity of the ResNet model were 100% and 100%, respectively, because the ResNet model can correctly detect all 1,000 non-COVID-19 images. The efficiency of ResNet indicates that the complex structure affects the learning process in deep learning. The precision and specificity of the MD-CNN model (96.60% and 96.69%) were slightly lower than the ResNet model. The precision and specificity of the AlexNet model (86.20% and 83.86%) were the least efficient.

To compare the proposed MD-CNN model with the previous work that studied COVID-19 detection on X-ray images, the results of each study are shown in Table 2. Narin compared ResNet50, ResNet101, ResNet152, InceptionV3, and Inception-ResNetV2, and found that ResNet50 was the best model in terms of accuracy (96.1%) and F1-score (83.50%).[18] Medhi developed a CNN

Table 2. Comparative analysis of previous works.

Author	Image	Method	Accuracy	F1- score	AUC
Narin 2020[18]	341 COVID-19, 2,800 healthy	ResNet50	96.10	83.50	-
Medhi 2020[19]	14,000 images	CNN	93.00	-	-
Apostolopoulos 2020[20]	700 COVID-19, 1,204 healthy	VGG 19	98.75	-	-
Guefrechi 2021[21]	623 COVID-19, 3,000 healthy	VGG 16	98.30	98.00	-
Akter 2021[22]	26,000 COVID-19, 26,000 healthy	Modified MobileNetV2	98.00	97.00	-
Ismael 2021[23]	180 COVID-19, 200 healthy	ResNet50 Features + SVM	94.74	94.79	0.99
Our proposed	10,000 COVID-19, 10,000 healthy	MD-CNN	97.95	97.92	0.98

architecture with two blocks of two convolutional layers followed by max pooling layers using ReLu function, a kernel size equal to 3x3 in the feature extraction section, and a fully connected layer consisting of a flatten layer and a Softmax activation layer.[19] The accuracy of the CNN was 93.00%. Apostolopoulos compared VGG19, MobileNet v2, Inception, Xception, and Inception ResNet v2, and found that the accuracy of VGG19 was the highest (98.75%).[20] Guefrechi evaluated three models (VGG16, ResNet50, and InceptionV3), and found that VGG16 had the best efficiency in accuracy for COVID-19 prediction, with an accuracy of 98.30% and an F1-score of 98.00%.[21] Akter selected several models to experiment on COVID-19 detection, including VGG19, VGG16, InceptionV3, ResNet50, ResNet101, GoogleNet, MobileNet, AlexNet, EfficientNet B7, DenseNet121, NFNet, and compared the developed approach (Modified MobileNetV2).[22] Modified MobileNetV2 had the best accuracy (98.00%) and F1-score (97.00%). Ismael developed a hybrid deep learning (ResNet50 model) and machine learning (Support Vector Machine: SVM) and compared the performance with Fine-tuning of ResNet50, End-to-end training of CNN, and the Binarized Statistical Image Features (BSIF)+SVM. The ResNet50+SVM had the best accuracy in training (94.74%), F1-score (94.79%), and 0.99 AUC.[23]

The comparison indicates that the accuracy of several works was lower than our work, while the accuracy of several works was similar to our study. Several studies in Table 2 used a small dataset size, which is important to note as it may lead to overfitting.[18-23]

Limitations

The limitation of this work is the concern of the overfitting problem. Overfitting is a common pitfall in deep learning where small training data size, a long time of training on a single set of data, noise data with a large amount of irrelevant information, or a complex model can lead to inaccurate predictions. The way to avoid overfitting is by using a large number of datasets, adding weight regularization, and dropping out.

In this study, we used 20,000 images compared to the data of previously published work, and the number of images used in this study is larger than several works.[18,21,23] However, this may still cause overfitting. In the case of using a small dataset, overfitting can be treated by image augmentation.

Image augmentation is a method of increasing the image dataset by varying the characteristics of the image such as reflection, rotation, scaling, shearing, and translation. In the case of chest X-rays, the structure of the lung is complex, and image augmentation may not help to improve the performance of prediction. Elgendi *et al.* reported that the use of geometrical image augmentation in X-ray images may not be effective for detecting COVID-19.[24] The accuracy of COVID-19 prediction with augmentation was 93.42%, while the accuracy of COVID-19 prediction without augmentation was 97.95%. The pattern of the chest image is an important factor for image augmentation. Therefore, it is necessary to choose a suitable technique for the lung organ.

Another very important factor is dropout, which is a regularization method that can help reduce irrelevant image data. Our work set two dropouts at 20% in the fully connected layers, after a dense layer. Tan *et al.*[25] studied the effect of different dropout percentages on training accuracy, comparing dropout rates of 20%, 40%, 60%, and 80%. The results showed higher training accuracy for 20%, 40%, and 60% dropout rates, while 80% resulted in lower training accuracy. Dropout rates of 20% and 40% resulted in lower training loss, while a 60% dropout rate resulted in high training loss, and an 80% dropout rate resulted in the highest training loss.

The image resolution of the input image is another overfitting parameter. In this work, the input image had a size of 250x250 pixels, which is a large image matrix size. The image size influences the learning of the model, with larger sizes being more prone to overfitting than smaller sizes.[26] Therefore, the large image matrix size affects the training time. However, a high resolution can improve the performance of image classification.[27,28]

Conclusion

In conclusion, the classification of chest X-ray images to distinguish between COVID-19 and non-COVID-19 cases is a challenging task. In this study, we developed a deep learning model based on the modified deep convolutional neural network (MD-CNN) architecture, which demonstrated superior performance compared to the ResNet and AlexNet models. Our proposed MD-CNN achieved a classification accuracy of 97.95%, highlighting its potential as an effective tool for COVID-19 diagnosis. However, the limited size of the dataset used in this study could be a potential limitation.

The results of this study also suggest that overfitting can be a significant issue when working with a small dataset, and techniques such as image augmentation may

be necessary to address this challenge. Future work could focus on exploring other deep learning architectures or ensemble methods to further improve the accuracy of COVID-19 diagnosis. Additionally, efforts to collect larger and more diverse datasets of chest X-ray images could enable the development of even more robust models for COVID-19 diagnosis.

Conflict of interest

None

Funding

The study was supported by Naresuan University (NU), and National Science, Research, and Innovation Fundamental Fund (NSRF). Grant NO. (R2565B090).

Ethical Approval

The study was approved by the ethics committee of Naresuan University, Thailand (IRB No. P10111/64).

References

[1] World Health Organization. Weekly epidemiological update on COVID-19-13 April 2023. Geneva: WHO. [cited 2022 April 30]. Available from: https://www.who.int/publications/m/item/weekly-epidemiological-update-on-covid-19-13-april-2023. Published 2022.

[2] World Health Organization. Use of SARS-CoV-2 antigen-detection rapid diagnostic tests for COVID-19 self-testing. Geneva: WHO. [cited 2022 April 28]. Available from: https://www.who.int/publications/i/item/WHO-2019-nCoV-Ag-RDTs-Self_testing-2022.1

[3] Adarve Castro A, Díaz Antonio T, Cuartero Martínez E, *et al*. Usefulness of chest X-rays for evaluating prognosis in patients with COVID-19. Radiologia. 2001; 63: 476-83.

[4] Cleverley J, Piper J, Jones MM. The role of chest radiography in confirming covid-19 pneumonia, BMJ 2020; 370: m2426. doi: 10.1136/bmj.m2426

[5] Borkowski AA, Viswanadhan NA, Thomas LB, *et al*. Using Artificial Intelligence for COVID-19 Chest X-ray Diagnosis. Fed Pract. 2020; 37(9): 398-404. doi: 10.12788/fp.0045.

[6] Masud R, Al-Rei M, Lokker C. Computer-Aided Detection for Breast Cancer Screening in Clinical Settings: Scoping Review. JMIR Med Inform. 2019; 7(3): e12660. doi: 10.2196/12660.

[7] Fehr J, Konigorski S, Olivier S, *et al*. Computer-aided interpretation of chest radiography reveals the spectrum of tuberculosis in rural South Africa. npj Digit. Med. 2021;4:106. doi.org/10.1038/s41746-021-00471-y

[8] Wang S, Cao G, Wang Y, *et al*. Review and prospective: artificial intelligence in advanced medical imaging. Front Radiol. 2021; 1: 1-18.

[9] Li Q, Cai W, Wang X, *et al*. Medical image classification with convolutional neural network. Proceedings of the 2014 13th International Conference on Control Automation Robotics & Vision (ICARCV), December 2014, 844-8, Singapore, 2014.

[10] Asada N, Doi K, MacMahon H, *et al*. Potential usefulness of an artificial neural network for differential diagnosis of interstitial lung diseases: pilot study. Radiology. 1990; 177(3): 857-60.

[11] Reshi AA, Rustam F, Mehmood A, et al. An Efficient CNN Model for COVID-19 Disease Detection Based on X-Ray Image Classification. Complexity. 2021, Article ID 6621607. doi.org/10.1155/2021/6621607

[12] Kanjanasurat I, Tenghongsakul K, Purahong B, *et al*. CNN–RNN Network Integration for the Diagnosis of COVID-19 Using Chest X-ray and CT Images. Sensors 2023, 23, 1356. doi.org/10.3390/s23031356

[13] Joshua EH. Convolutional Neural Network for COVID-19 Detection in Chest X-Rays. 2022. Honors Thesis. 254. Available from: https://red.library.usd.edu/honors-thesis/254

[14] Pandey N. Lung segmentation from Chest X-Ray Mask and Lables. Kaggle Inc [cited 2022 April 28]. Available from: https://www.kaggle.com/datasets/nikhilpandey360/chest-xray-masks-and-labels

[15] Pandey N. Lung segmentation from Chest X-Ray dataset. Kaggle Inc [cited 2022 April 28]. Available from: https://www.kaggle.com/code/nikhilpandey360/lung-segmentation-from-chest-x-ray-dataset/notebook

[16] COVID-19 Radiography Database. Kaggle Inc. [cited 2022 April 28]. Available from: https://www.kaggle.com/datasets/tawsifurrahman/covid19-radiography-database. Published 2022.

[17] Google collaborators. Google Research. [cited 2022 April 28]. Available from: www.google colaboratory.com

[18] Narin A, Kaya C, Pamuk Z. Automatic detection of coronavirus disease (COVID-19) using X-ray images and deep convolutional neural networks. Pattern Anal Appl. 2021; 24: 1207-20. doi.org/10.1007/s10044-021-00984-y

[19] Jamil MK, Iftekhar Hussain. Automatic Detection of COVID-19 Infection from Chest X-ray using Deep Learning. medRxiv preprint doi: doi.org/10.1101/2020.05.10.20097063

[20] Apostolopoulos ID, Mpesiana TA. Covid-19: automatic detection from X-ray images utilizing transfer learning with convolutional neural networks. Phys Eng Sci Med. 2020; 43: 635-40. doi.org/10.1007/s13246-020-00865-4.

[21] Guefrechi S, Jabra MB, Ammar A, *et al*. Deep learning based detection of COVID-19 from chest X-ray images. Multimed Tools Appl. 2021; 80: 31803-20. doi.org/10.1007/s11042-021-11192-5

[22] Akter S, Javed Mehedi Shamrat FM, Chakraborty S, *et al*. COVID-19 Detection Using Deep Learning Algorithm on Chest X-ray Images. Biology 2021; 10: 1174. doi.org/10.3390/biology10111174

[23] Ismael AM, Şengür A. Deep learning approaches for COVID-19 detection based on chest X-ray images. Expert Syst Appl. 2021; 114054. doi.org/10.1016/j.eswa.2020.114054

[24] Elgendi M, Nasir MU, Tang Q, *et al*. The Effectiveness

of Image Augmentation in Deep Learning Networks for Detecting COVID-19: A Geometric Transformation Perspective. Front. Med. 2021; 8: 629134. doi: 10.3389/fmed.2021.629134

[25] Tan SZK, Du R, Perucho JAU, Chopra SS, *et al*. Dropout in Neural Networks Simulates the Paradoxical Effects of Deep Brain Stimulation on Memory. Front. Aging Neurosci. 2020; 12: 273. doi: 10.3389/fnagi.2020.00273

[26] Rukundo O. Effects of image size on deep learning. Available from: https://arxiv.org/ftp/arxiv/papers/2101/2101.11508.pdf

[27] Sabottke CF, Spieler BM. The effect of image resolution on deep learning in radiology. Radiol Artif Intell. 2020; 2(1): e190015. doi.org/10.1148/ryai.2019190015

[28] Thambawita V, Strümke I, Hicks SA, *et al*. Impact of image resolution on deep learning performance in endoscopy image classification: An experimental study using a large dataset of endoscopic images. Diagnostics. 2021; 11(12): 2183. doi.org/10.3390/diagnostics11122183